Acta Pharmaceutica Sinica B 2021;11(7):2031–2047

Chinese Pharmaceutical Association
Institute of Materia Medica, Chinese Academy of Medical Sciences

Acta Pharmaceutica Sinica B

www.elsevier.com/locate/apsb
www.sciencedirect.com

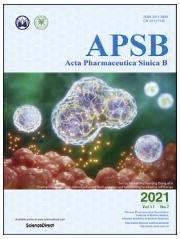

ORIGINAL ARTICLE

Intranasal temperature-sensitive hydrogels of cannabidiol inclusion complex for the treatment of post-traumatic stress disorder

Lulu Pang[a,b,†], Siqing Zhu[a,c,†], Jinqiu Ma[a,b], Lin Zhu[a], Yijing Liu[a,b], Ge Ou[a,d], Ruiteng Li[a,b], Yaxin Wang[e], Yi Liang[e], Xu Jin[e,*], Lina Du[a,b,c,*], Yiguang Jin[a,c,*]

[a]*Department of Pharmaceutical Sciences, Beijing Institute of Radiation Medicine, Beijing 100850, China*
[b]*College of Pharmacy, Shandong University of Traditional Chinese Medicine, Jinan 250355, China*
[c]*College of Pharmacy, Anhui Medical University, Hefei 230001, China*
[d]*Pharmacy Department, Chinese PLA General Hospital, Beijing 100853, China*
[e]*Department of Anesthesiology, Beijing Tiantan Hospital, Capital Medical University, Beijing 100070, China*

Received 12 October 2020; received in revised form 15 December 2020; accepted 6 January 2021

KEY WORDS

Post-traumatic stress disorder;
Cannabidiol;
Hydroxypropyl-β-cyclodextrin;
Inclusion complex;
Hydrogels;
Brain targeting;
Blood–brain barrier;
Intranasal administration

Abstract Post-traumatic stress disorder (PTSD) is a psychiatric disease that seriously affects brain function. Currently, selective serotonin reuptake inhibitors (SSRIs) are used to treat PTSD clinically but have decreased efficiency and increased side effects. In this study, nasal cannabidiol inclusion complex temperature-sensitive hydrogels (CBD TSGs) were prepared and evaluated to treat PTSD. Mice model of PTSD was established with conditional fear box. CBD TSGs could significantly improve the spontaneous behavior, exploratory spirit and alleviate tension in open field box, relieve anxiety and tension in elevated plus maze, and reduce the freezing time. Hematoxylin and eosin and c-FOS immunohistochemistry slides showed that the main injured brain areas in PTSD were the prefrontal cortex, amygdala, and hippocampus CA1. CBD TSGs could reduce the level of tumor necrosis factor-α caused by PTSD. Western blot analysis showed that CBD TSGs increased the expression of the 5-HT1A receptor. Intranasal administration of CBD TSGs was more efficient and had more obvious brain targeting effects

Abbreviations: AUC, area under the curve; BBB, blood–brain barrier; CBD TSGs, cannabidiol inclusion complex temperature-sensitive hydrogels; CNS, central nervous system; COVID-19, coronavirus disease 2019; DSC, differential scanning calorimetry; HP-β-CD, hydroxypropyl-β-cyclodextrin; IR, infrared; IS, internal standard; MRM, multiple reaction monitoring; PPV, percentage of persistent vibration; PTSD, post-traumatic stress disorder; PVD, persistent vibration duration; SSRIs, selective serotonin reuptake inhibitors; TNF-α, tumor necrosis factor-α; WB, Western blot.

*Corresponding authors.
E-mail addresses: jxsys2020@gmail.com (Xu Jin), dulina@188.com (Lina Du), jinyg@sina.com (Yiguang Jin).

†These authors made equal contributions to this work.

Peer review under the responsibility of Chinese Pharmaceutical Association and Institute of Materia Medica, Chinese Academy of Medical Sciences.

https://doi.org/10.1016/j.apsb.2021.01.014

than oral administration, as evidenced by the pharmacokinetics and brain tissue distribution of CBD TSGs. Overall, nasal CBD TSGs are safe and effective and have controlled release. There are a novel promising option for the clinical treatment of PTSD.

1. Introduction

Post-traumatic stress disorder (PTSD) is a tardive, long-term mental disorder of individuals after suffering an abnormal catastrophic event[1]. PTSD patients usually enczounter or witness an extreme scenario of death in corona virus disease 2019 (COVID-19), war, earthquakes, and so on[2]. Once PTSD occurs, symptoms such as nausea, diarrhea, accelerated heart rate[3], sleep disorders[4] and depression[5], which seriously affect quality of life and work[6]. Patients' suicidal tendencies are also higher than those of ordinary persons[7]. The brain is the main organ affected by PTSD[8]. PTSD can seriously affect brain function[9], and the excessive stress response causes the brain structure and function to exceed a certain tolerance range, resulting in the failure of information memory of the central nervous system[10].

The clinical treatment of PTSD is mainly based on psychological therapy and medical therapy. At present, there are no medicines specifically for the treatment of PTSD. SSRIs, such as sertraline, paroxetine, and fluoxetine[11], which are used to treat depression clinically[12], are also used to treat PTSD. As a result, sertraline is usually chosen as the positive control in pharmacodynamic experiments[13]. However, the disadvantages of oral medicine include low treatment efficacy, the first-pass effect and gastrointestinal irritation. Therefore, the development of a safe, effective and controlled release formulation for the treatment of PTSD has become a vital target.

Cannabidiol (CBD) is the main component extracted from cannabis without addiction[14] (Fig. 1). CBD has a wide range of pharmacological effects, including anti-inflammation[15], neuroprotection[16], immunomodulation[17] and anti-anxiety effects[18]. It has therapeutic potential in many diseases such as epilepsy[19], neurodegeneration[20], and schizophrenia[21]. Moreover, the U.S. Food and Drug Administration (FDA) has approved the liquid formulation of CBD for the treatment of epilepsy. As one of the components of cannabis, CBD can act on the CB1[22] and CB2[23] receptors of the endocannabinoid system (ECS) to stimulate the ECS to promote sleep quality, prevent the generation of traumatic memories, and establish physical and emotional senses of well-being. Therefore, CBD can reduce the destructive symptoms of PTSD and alleviate the emotions of fear and depression[24]. CBD can work faster and has fewer side effects for PTSD treatment than SSRIs, which start to work after several weeks and have side effects such as insomnia, restlessness, and sexual dysfunction[25].

To date, the treatment of brain diseases is still an important topic all over the world[26]. Owing to the existence of the blood–brain barrier (BBB)[27], it is difficult for medicines to penetrate or bypass the BBB by the traditional peripheral administration methods[28], and it is hard to reach an effective therapeutic concentration in the central nervous system (CNS)[29].

Intranasal administration is known as a novel delivery strategy to penetrate or bypass the BBB[30]. Moreover, the olfactory nerve pathway[31], the olfactory epithelial cell pathway[32] and the trigeminal nerve pathway are the important routes for medicine to enter the brain by bypassing the BBB. Long-term maintenance of topical formulations is the key for high absorption and high bioavailability of medicine, and bioadhesive formulations are the

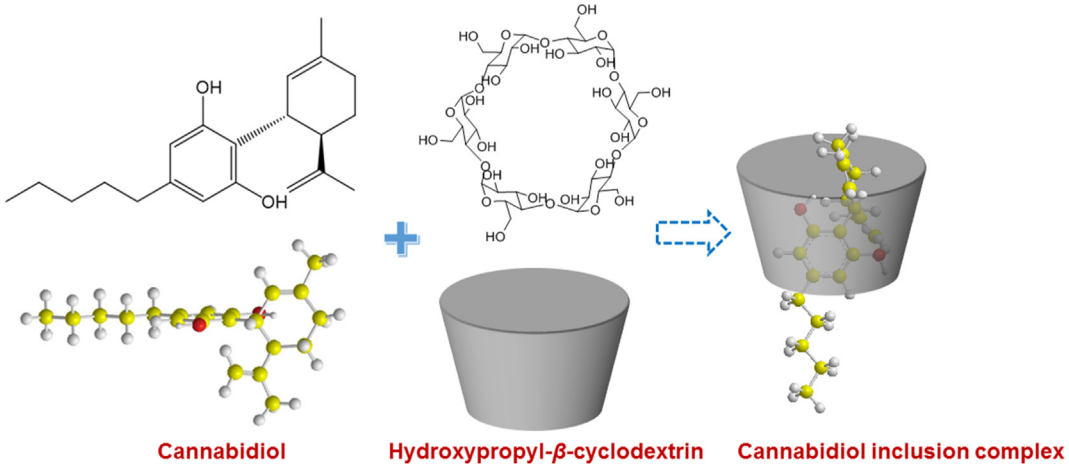

Figure 1 Chemical structure of cannabidiol (CBD) and the formation scheme of CBD inclusion complex.

most appropriate solution method. Temperature-sensitive hydrogels are a preparation that can immediately undergo a phase transition at the application site from the solution state into the semisolid gel state[33].

In this study, a CBD inclusion complex was prepared first to improve the solubility of CBD (Fig. 1). Then, temperature-sensitive hydrogels (CBD TSGs) were formulated with poloxamers as the temperature-sensitive polymers. The advantages of CBD TSGs include the prevention of nasal cilia clearance, long retention time in the nasal cavity and increased bioavailability. Nasal administration can increase the distribution of CBD in the brain and achieve excellent anti-PTSD effects.

2. Materials and methods

2.1. Materials

The chemicals and their commercial sources were as follows: cannabidiol (purity>98%, Yunnan Hansu Biotechnology Co., Ltd., Kunming, China); hydroxypropyl-β-cyclodextrin (Zhongqi Pharmaceutical Technology Co., Ltd., Shijiazhuang, China); *tert*-butyl alcohol, potassium chloride and heparin sodium (Sinopharm Chemical Reagent Co., Ltd., Shanghai, China); poloxamer 188 and poloxamer 407 (Beijing Fengli Jingqiu Trading Co., Ltd., Beijing, China); sodium chloride (Xilong Science Co., Ltd., Shantou, China); calcium chloride (Beijing Modern Oriental Fine Chemical Co., Ltd., Beijing, China); sodium deoxycholate (China PharmaceuticalCompany, Shanghai, China); MD44 dialysis bag with a cutoff molecular weight of 3500 Da (Beijing Solarbio Technology Co., Ltd., Beijing, China); paraformaldehyde (Alfa Aesar Chemical Co., Ltd., Shanghai, China); mouse TNF-α ELISA kit (Neobioscience Co., Ltd., Shenzhen, China); dimethyl sulfoxide (Aladdin Reagent Co., Ltd., Shanghai, China); propranolol (Wuhan Kanuosi Technology Co., Ltd., Wuhan, China); isoflurane (Ruiward Life Technology Co., Ltd., Shenzhen, China); and methanol, acetonitrile and formic acid of chromatographic purity (Thermo Fisher Scientific Co., Ltd., New York, NY, USA).

2.2. Animals

Toads (60−80 g, male) were obtained from Jiaxiang Huarong Breeding Professional Cooperation (Jining, China). A sheep head of 2.0 kg was purchased from Dachengshuangying Market (Beijing, China).

C57BL/6N mice [19−21 g, SPF, License number: SCXK (Beijing) 2016−0006] were purchased from the Vital River Laboratory Animal Technology Co., Ltd. (Beijing, China). The mice were bred at 21−25 °C with 12 h light/12 h dark cycles (lights on at 8:00 am), and they had free access to food and water. All experimental procedures were executed according to the protocols approved by China Animal Care and Use Committee. Animal test was approved by the Ethical Committee of Academy of Military Medical Sciences.

2.3. HPLC measurement

CBD was evaluated using an HPLC system (Agilent 1260, Palo Alto, CA, USA) with a Diamonsil C18 column. The mobile phase was methanol:water = 85:15 (*v*/*v*) with a detection wavelength of 220 nm, a column temperature of 30 °C, a flow rate of 1.0 mL/min, and an injection volume of 10 μL[34].

2.4. Preparation of CBD TSGs

2.4.1. Preparation of the CBD inclusion complex

CBD and hydroxypropyl-β-cyclodextrin (HP-β-CD) were dissolved in *tert*-butyl alcohol and ultrapure water, respectively. Then, the CBD solution was slowly added to the HP-β-CD solution with magnetic stirring[35]. Then, the mixed solution was lyophilized in a freeze dryer (LGJ-30, Beijing Songyuan Huaxing Technology Co., Ltd., Beijing, China) for 42 h.

2.4.2. Preparation of CBD TSGs

Poloxamer 188 (2 g) and 407 (12 g) were mixed in a 50 mL beaker, 30 mL of water was added, and the mixture was swelled at 4 °C for 48 h. Finally, blank TSGs were obtained with the final volume of 50 mL[36]. The lyophilized CBD inclusion complex was added to the blank TSGs with a final CBD concentration of 30 mg/mL. Transparent CBD TSGs were acquired finally with the CBD inclusion complex completely dissolved.

2.5. Characterization of CBD inclusion complex

For the solubility determination, excess CBD was added to 0, 5, 10, 15, 20, 25, and 30 mmol/L HP-β-CD aqueous solutions and agitated with 120 rpm at 37 °C for 72 h. Then, the concentration of CBD in the HP-β-CD solutions was measured by HPLC. The phase solubility curves of the HP-β-CD concentration (*X* axis) *versus* CBD concentration (*Y* axis) were plotted to determine the inclusion types. The morphology of the CBD inclusion complex was observed under SEM (HITACHI S4800, Tokyo, Japan).

The inclusion rate is an important index to evaluate the preparation of the inclusion complex. The CBD inclusion complex was washed with ethanol three times to remove noninclusion CBD and dried at 40 °C. Then, the samples were dissolved in methanol to determine the CBD content, and the calculation of the inclusion rate of CBD inclusion complex as shown in Eq. (1)[37].

$$\text{Inclusion rate (\%)} = \text{Actual CBD in inclusion complex/Total CBD} \times 100 \quad (1)$$

The infrared spectrum of CBD, HP-β-CD, the CBD-HP-β-CD inclusion complex and their physical mixture were determined at 4000–600 cm^{-1} by a flourier infrared (IR) spectrometer (Spectrum TWO, PerkinElmer Enterprise Management Co., Ltd., Shanghai, China)[38]. At the same time, the differential scanning calorimetry (DSC) curves of the samples were measured at 50−300 °C by a differential scanning calorimeter (DSC-500T, Yanjin Scientific Instrument Co., Ltd., Shanghai, China)[39].

2.6. Characterization of CBD TSGs

The gelation temperature and gelation time of CBD TSGs were determined by the test tube inversion method[40]. CBD TSGs of 2 mL were placed in the test tube and put in a water bath with constant temperature (HH-2, Zhiborui Instrument Manufacturing Co., Ltd., Changzhou, China). The temperature was slowly increased from 20 to 40 °C with the rate of 1 °C/min. The test tube was inverted and the flowing condition of CBD TSGs was observed. The temperature was recorded as the gelation temperature when the liquid was not flowable, and the time when it changed from a solution to a semi-solid state was recorded as the gelation time.

The changes in the storage modulus (G′), loss modulus (G″) and viscosity (η) of CBD TSGs were investigated with an advanced rotational rheometer (MCR301, Anton Paar Co., Ltd., Graz, Austria). At the same time, the changes in the modulus and viscosity at nasal temperature (34 °C) within a range of 0.1−100 rad/s were also measured[40].

For the *in vitro* release of CBD TSGs, an HPLC method was established first. The retention time of CBD was 7.588 min, and the peak shape was good. The linear relationship of CBD was good with a linear regression equation of $A = 40.127C + 51.826$ ($r = 0.9999$) and a linear range of 10−200 μg/mL. CBD TSGs (10 mg/mL, 1 mL) were added first to the pretreated dialysis bag with a cutoff molecular weight of 3500, which was then placed into a centrifuge tube containing 50 mL of 20% (*w*/*v*) ethanol solution. The centrifuge tube was maintained at 37 °C with an agitation speed of 200 rpm (THZ-D, Taicang Experimental Instrument Co., Ltd., Taicang, China). To evaluate the release profiles *in vitro*, 1 mL samples were taken out at 0.25, 0.5, 1, 2, 4, 6, 8, 10, 12, 24, 36, and 48 h, and the dissolution medium (37 °C, 1 mL) was supplemented[41]. All the samples were analyzed by HPLC, and the calculation of the cumulative release (Q_n) of CBD as shown in Eq. (2):

$$Q_n = \frac{C_n \cdot V + V_0 \sum_{i=1}^{n-1} C_i}{A} \quad (2)$$

where Q_n (%) is the cumulative release rate, C_n (μg/mL) is the medicine concentration of sample n, C_i is the medicine concentration (μg/mL) of sample i, V (mL) is the volume of the dissolution medium, V_0 (mL) is the withdrawn volume, and A is the permeation area of CBD TSGs (cm^2). Finally, the Q_n–t release curve was plotted.

The transmucosa test was carried out with vertical Franz diffusion cells. 100 μL of artificial nasal fluid and 100 μL of 10 mg/mL CBD TSGs were added to the supply chamber, and the receptor chamber was filled with physiological saline (PS). Then, they were maintained at 36.5 °C with a stirring rate of 300 rpm 1 mL samples were taken out at 0.5, 1, 2, 3, 4, 5, and 6 h, followed by supplementation with the release medium at the same volume and temperature. The CBD content of the samples was determined by HPLC, and the cumulative permeation amount of CBD was calculated, which was similar to the release test *in vitro*.

The irritation caused by CBD TSGs was evaluated by the gold standard-the cilia swing evaluation of a toad's palate[42]. In detail, the morphological changes and the lasting time of ciliary movement (LTCM) of toads isolated to the upper palate mucosa were observed after they were treated with different samples, including PS (negative control), 1% sodium deoxycholate (positive control), blank TSGs, a CBD TSGs at 10, 20, and 30 mg/mL. Palates were excised with a surgical blade after the toads were decapitated. The palate mucous membrane (3 mm × 3 mm) was separated and washed with PS. The pilus sides were spread onto the glass slides. An aliquot (0.1 mL) of the different samples was dropped onto the pilus. Slides were placed into a tightly closed container full of PS. The oscillation status of the pilus was observed under a microscope (BDS200-FL, Chongqing Optec Instrument Co., Ltd., Chongqing, China) until oscillation stopped. When the oscillation of the pilus stopped, the mucosa was thoroughly washed with PS and observed again. If the oscillation recovered, the time was recorded as the LTCM after recovery. The total duration time of continuous oscillation of the cilia was defined as the sum of the measured total LTCMs. The percentage of relative ciliary movement was defined according to Eq. (3). The lower the value is, the more obvious toxicity to the ciliary samples.

Percentage of relative ciliary movement (%) = Total ciliary oscillation time of samples/total ciliary oscillation time of PS × 100 (3)

2.7. Therapeutic effects of CBD TSGs on PTSD mice

2.7.1. Model establishment of PTSD and administration scheme

The establishment of the PTSD model was divided into two stages. First, C57 mice were placed in a conditional fear box (DigBehv, Shanghai Jiliang Software Technology Co., Ltd., Shanghai, China) to move freely for 300 s. Then, an electric shock was performed with an electrical current of 0.8 mA for 10 s and a 10 s interval for a total 15 cycles. The stimulation was continued for two days[43]. The healthy mice were placed in the conditional fear box for 600 s without any operation. More importantly, 75% alcohol was sprayed to eliminate the influence of feces, urine and smell from the previous animal.

Seventy male C57 mice were randomly divided into 7 groups with 10 mice in each group, including the healthy group, the model group, the blank TSGs group, the positive control of oral sertraline tablets group (6.5 mg/kg), and the low- (10 mg/kg), medium- (20 mg/kg) and high-dose (30 mg/kg) CBD TSGs groups. The mice were administered different prescriptions at 1 h after the establishment of PTSD. The positive control mice were administered 0.2 mL of an oral sertraline suspension, and the nasal administration groups were given 20 μL of blank or CBD TSGs once a day for 10 consecutive days. The healthy group and the model group did not receive any treatment (Fig. 2).

2.7.2. Spontaneous behavior of PTSD mice evaluated by the open field test

An open field instrument (DB018, Zhishu Duobao Biotechnology Co., Ltd., Beijing, China) was used to evaluate the autonomic responses, exploratory behavior and stress of the mice in a new environment. All mice were placed in the central area at the bottom on the Day 8 after administration. The attached software recorded the time and movement videos automatically within 5 min.

2.7.3. Anxiety of the PTSD mice evaluated by the elevated plus maze

The elevated plus maze (DB015, Zhishu Duobao Biotechnology Co., Ltd.,) can evaluate the anxiety state of the animals. On the Day 9 after administration, the mice were placed at the central area of the elevated plus maze, and the software recorded the time and movement videos automatically within 5 min[44].

2.7.4. Feared state of PTSD mice assessed with the freezing behavior test

The freezing behavior test is performed in a conditional fear box (Shanghai Jiliang Software Technology Co., Ltd.). On Day 10 after administration, the mice were placed in the conditional fear box, and the freezing time within 5 min was recorded.

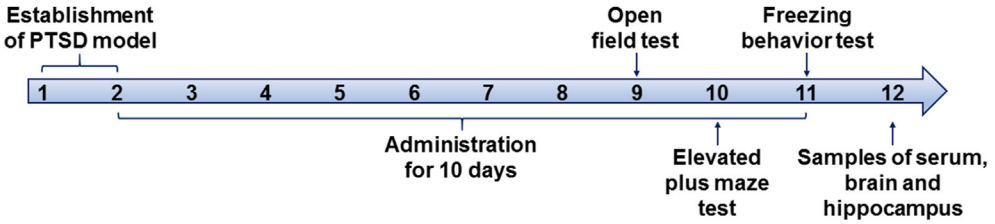

Figure 2 Administration scheme and the therapeutic schedule.

2.7.5. Pathological observations and expression of TNF-α and the 5-HT1A receptor in PTSD mice

After 10 days of administration, the mice were sacrificed, the whole brain was stripped out on ice and immersed in 4% paraformaldehyde for one week. H&E staining and c-FOS immunohistochemistry were performed on the prefrontal cortex, hippocampus and amygdala area as the major observed areas[45].

After the behavioral evaluation, 1 mL of blood was taken and centrifuged at 4 °C at 4000×*g* for 10 min to obtain serum (Desktop freezing centrifuge, Fresco 21, Thermo Fisher Scientific Co., Ltd.). Then, the amount of TNF-α in the serum was measured according to the standard protocol of the ELISA kit.

The mice were sacrificed after administration for 10 days. Hippocampal tissues were stripped on ice to detect the expression of the 5-HT1A receptor with Western blot (WB) according to the related standard protocol[46].

2.8. Pharmacokinetics and tissue distribution of CBD TSGs by oral and nasal administration

2.8.1. Mass spectrometry and chromatography methods to detect CBD content

An LC-20AD liquid phase (Shimadzu, Japan) tandem API 5000 liquid–mass spectrometry system was used to determine the CBD content. In this study, propranolol was used as the internal standard (IS), and multiple reaction monitoring (MRM) scanning was used to detect the positive ionization mode. The detailed detection condition included collision gas at 8 psi, curtain gas at 20 psi, ion source gas 1 at 50 psi, ion source gas 2 at 80 psi, an ion spray voltage of 5500 V, and an ion source temperature of 550 °C.

A Phenomenex C18 column (50 mm × 3.0 mm, 2.6 μm) was used. The mobile phase consisted of 0.1% formic acid aqueous solution (A) and 0.1% formic acid acetonitrile solution (B) with a flow rate of 0.8 mL/min. The gradient elution was as follows: 10% B from 0.0 to 0.3 min, 10%−95% B from 0.3 to 1.0 min, 95% B from 1.0 to 2.0 min, 95%−10% B from 2.0 to 2.1 min, and 10% B from 2.1 to 3.0 min. The temperature of column was maintained at 40 °C with an injection volume of 5 μL[47].

2.8.2. Standard curves of CBD in plasma, brain and liver

CBD stock solution at a 10 mg/mL concentration was diluted with methanol to final concentrations of 50, 100, 200, 500, 1000, 2000, 5000, 10,000, and 20,000 ng/mL. The above-mentioned working solution of 5 μL each with different concentrations were added to blank plasma of 45 μL. The final concentrations of CBD in the plasma samples were 5, 10, 20, 50, 100, 200, 500, 1000, and 2000 ng/mL. The standard curves of CBD in the brain and liver were similar.

2.8.3. Pretreatment of the plasma, brain and liver samples

The direct protein precipitation method was used to prepare the plasma samples. 200 μL of propranolol acetonitrile solution (5 ng/mL) was added to 50 μL of blank plasma, brain or liver samples, vortexed for 30 s, and centrifuged at 4000×*g* and 4 °C for 10 min (Desktop freezing centrifuge, Thermo Fisher Scientific Co., Ltd.). 60 μL of supernatant was mixed with 60 μL of purified water to be determined.

2.8.4. Pharmacokinetics and tissue distribution of CBD TSGs by oral and nasal administration

Twelve male and twelve female C57 mice were randomly divided into the oral group and the nasal group, with 12 mice in each group (6 males and 6 females). The oral group was administered 0.2 mL of CBD suspension (60 mg of CBD was added to 20 mL of 0.5% (*w/v*) CMC-Na solution under magnetic stirring to make a homogeneous suspension). The nasal administration group was administered 20 μL of CBD TSGs (30 mg/mL) by unilateral nasal administration. All the administration doses were 30 mg/kg. Plasma from the mice was collected through the orbital venous plexus. The 12 mice were divided into two batches randomly, and the two batches had blood collected alternately, which meant the two batches were evaluated one after another at the adjacent time points. Blood samples of 0.25 mL were taken from the orbit at 0.08, 0.25, 0.5, 1, 2, 4, 8, and 12 h after administration, placed into 1.5 mL centrifuge tubes, rinsed with heparin sodium solution, and centrifuged with 1800×*g* for 10 min at 4 °C (Desktop freezing centrifuge, Thermo Fisher Scientific Co., Ltd.).

Sixty C57 mice (30 males and 30 females) were randomly divided into the oral and the nasal administration group with 30 mice in each group (15 males and 15 females). The overall operation was similar to that of the pharmacokinetics test. The mice were sacrificed at 0.08, 0.25, 1, 4, and 12 h after dosing, and the brains and livers were isolated. Purified water was added to the samples with a ratio of tissue:water = 1:4 (*v/v*). Then, the above samples were homogenized with a high-speed disperser (D-1, Miccra Co., Ltd., Germany) and stored at −80 °C for further analysis.

In order to evaluate the distribution of CBD *in vivo*, the relative bioavailability (F) in blood, brain and liver were calculated according to Eq. (4):

$$F_{\text{blood/brain}}\,(\%) = \text{AUC}_{\text{nasal(blood/brain)}} / \text{AUC}_{\text{oral(blood/brain)}} \times 100 \quad (4)$$

2.9. Data analysis

The data are represented as the means ± SD. Statistical differences between groups were analyzed with one-way ANOVA. All statistical analyses were performed using SPSS software (19.0,

International Business Machines Corporation, Armonk, NJ, USA), $P < 0.05$ indicates statistical differences.

3. Results

3.1. Formation of CBD inclusion complex

Phase solubility is the most commonly used method to determine the inclusion constants and the inclusion ratios of drugs with cyclodextrins. The CBD concentration increased with the increase in the HP-β-CD concentration, which shows a positive correlation (Fig. 3A). This is in accordance with the solubility diagram of the A_L type phase, indicating that an inclusion complex with 1:1 M ratio was formed[48,49]. The inclusion complexes were loose porous slide solids observed under SEM (Fig. 3B).

Three methods to prepare the CBD inclusion complex were compared: milling, saturated aqueous solution and lyophilization. For the saturated aqueous solution method, most of the CBD precipitated and it could not form the inclusion complex efficiently. The water solubility of free CBD was only zero while that of the CBD inclusion complexes prepared with the milling and lyophilization methods were 1.02% (*w*/*v*) and 2.29% (*w*/*v*), respectively. The CBD inclusion complex that was prepared by the lyophilization method could improve the solubility of CBD slightly with an inclusion rate of 76.3%.

The IR spectrum is the standard to represent the formation of the inclusion complex. The typical hydroxyl vibration peaks of CBD were at 3408 and 3519 cm^{-1}, and the skeletal vibration of the benzene ring was at 1581 and 1623 cm^{-1}. The telescopic vibration peak of HP-β-CD hydroxyl was at 3403 cm^{-1}, and the telescopic vibration of the typical ether bond (C—O—C) was at 1023 cm^{-1}. In comparison, the IR spectrum of the CBD inclusion complex was almost as same as that of HP-β-CD with HP-β-CD peaks of 3403 and 1024 cm^{-1} without the representative peaks of CBD, which indicated that CBD had been enclosed completely in the HP-β-CD cavity. The IR spectrum of the physical mixture included both the characteristic peaks of CBD and HP-β-CD, which indicated that CBD was not entrapped in the cavity of HP-β-CD through simple physical mixing (Fig. 3C).

The peaks in DSC were also used to represent the formation of the CBD inclusion complex. In the DSC curve, CBD had a peak of approximately 65 °C, while HP-β-CD had a peak at 280 °C, which may be related to its thermal decomposition. In comparison, there were no peaks of the CBD inclusion complex at 65 and 280 °C and only a small peak at 180 °C, which may be caused by the hydrogen bonds formed during the inclusion process. These findings indicate that CBD has been completely incorporated in the HP-β-CD cavity. The physical mixture of CBD and HP-β-CD had peaks at approximately 65 and 240 °C, which is in accordance with their individual features (Fig. 3D).

3.2. Characteristics of CBD TSGs

The drug loading of the CBD TSGs was 12.8 ± 0.24%. The gelation temperature of CBD TSGs was 29.6 °C and the gelation time was 1.15 min. After nasal administration, the gels would likely rapidly form and the resident time of the gel on the nasal mucosa would highly increase.

The appearance of CBD TSGs at room temperature (25 °C) and nasal cavity temperature (34 °C) were flowable and gel-like, respectively (Fig. 4A). In the rheology evaluation, the storage modulus (G′) represents the semisolid-state, and the loss modulus (G″) represents the liquid state. When the temperature was 28 °C, the storage modulus G′ was equal to the loss modulus G″, which was the critical temperature for the transition from liquid to semisolid. When the temperature was lower than 28 °C, the loss

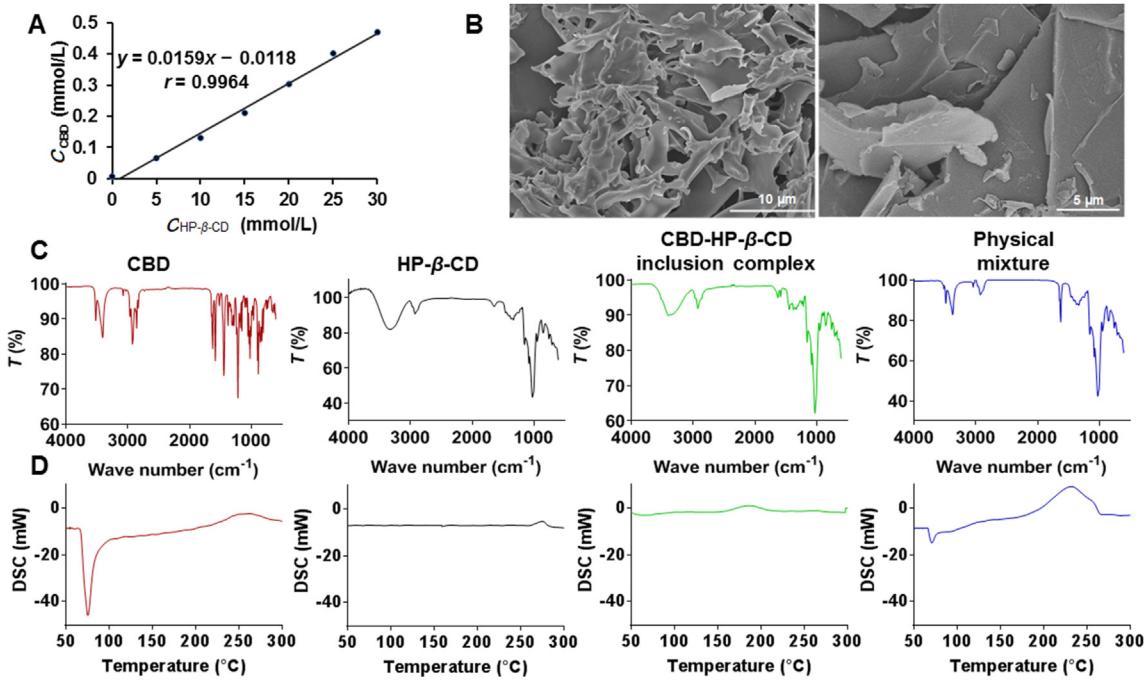

Figure 3 (A) Phase dissolution curve of CBD. The linear increase indicated that CBD and HP-β-CD formed an inclusion complex of A_L type. (B) Morphology of CBD inclusion complexes under SEM (scale bar = 10 and 5 μm). Infrared spectra (C) and DSC curves (D) of CBD, HP-β-CD, the CBD-HP-β-CD inclusion complex and their physical mixture.

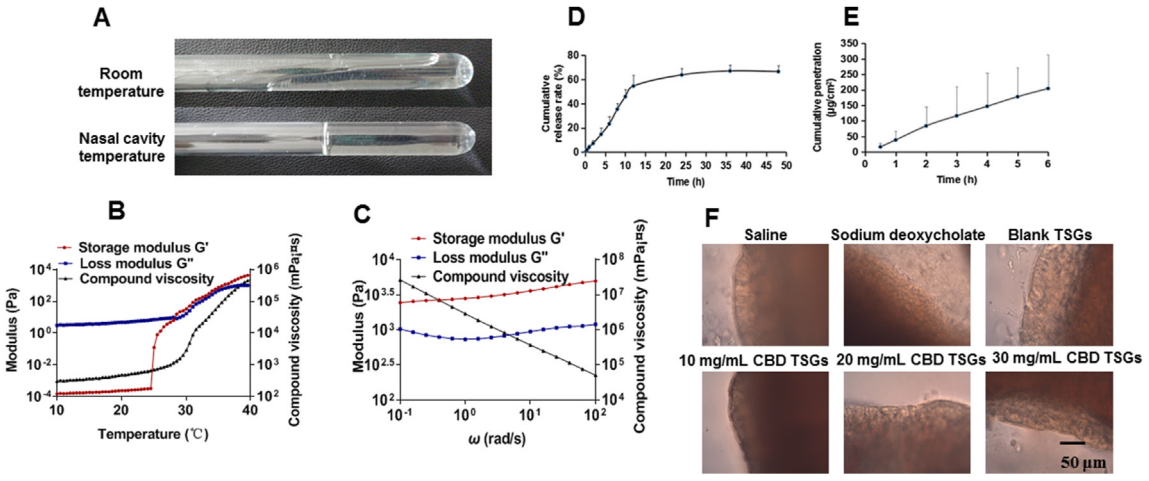

Figure 4 (A) The appearance of CBD TSGs at room temperature (25 °C) and nasal temperature (34 °C). (B) The profiles of the storage modulus (G′), the loss modulus (G″) and the compound viscosity of CBD TSGs at 10−40 °C with the oscillation frequency of 0.5 Hz, the strain amplitude of 0.05%, and the heating rate of 1 °C/min. (C) The profiles of storage modulus (G′), loss modulus (G″) and a compound viscosity of CBD TSGs at 0.1−100 rad/s with the nasal temperature of 34 °C and the strain rate of 0.05%. (D) *In vitro* release of CBD TSGs within 48 h. (E) The nasal mucosal permeability curve of CBD TSGs within 6 h. (F) The palate ciliary structure of toads treated with saline, sodium deoxycholate, blank TSGs and 10, 20, and 30 mg/mL CBD TSGs. Data are represented as mean ± SD ($n = 3$).

modulus G″ was higher than the storage modulus G′, which indicated that the CBD TSGs were a flowing liquid at this temperature. When the temperature was higher than 28 °C, the storage modulus G′ was greater than the loss modulus G″, which indicated that the CBD TSGs were semisolid and had gel elasticity at this temperature (Fig. 4B). This is advantageous for the nasal administration. At the temperature of the nasal cavity, CBD TSGs can adhere to the nasal mucosa, and the residence time will increase in the nasal cavity.

When the temperature was 34 °C (close to the nasal temperature) and the shear frequency (ω) was in the range of 0.1−100 rad/s, the storage modulus G′ was always greater than the loss modulus G″, which indicated that the semisolid property of the gels was stable. Furthermore, the viscosity of the gels decreased with the increased shear frequency. This shear thinning phenomenon indicated that the CBD TSGs had good syringe ability (Fig. 4C).

According to the Q_n–t curve, the CBD TSGs were completely released within approximately 12 h (Fig. 4D). The release mechanism is in accordance with the Ritger−Peppas equation (Table 1), which indicates the CBD release occurred *via* the synergistic effects of diffusion and matrix dissolution.

According to the Q_n–t curve, the cumulative permeation amount per unit area of CBD TSGs can reach approximately 200 μg within 6 h, and the pure CBD cannot penetrate the nasal mucosa (Fig. 4E).

The ciliary swing condition of the toad palate is the gold standard to evaluate the safety of nasal formulations[50]. For the negative PS group, the cilia were arranged neatly with the intact structure and active movement. This was similar to a wheat wave blown by the wind with a regular swing in the same direction and vibrant frequency. In comparison, the ciliary structure was severely damaged by 1% (*w*/*v*) sodium deoxycholate; part of the cilia fell off, the cilia of the mucosal surface were disordered and stopped swinging in a short time. Sodium deoxycholate as the positive group is well known to be highly irritating and toxic to the ciliary mucosa. The cilia of the blank TSGs and low- (10 mg/mL), medium- (20 mg/mL), and high-dose (30 mg/mL) CBD TSG groups were arranged neatly with complete structure and active movement. In addition, there was no cell shedding, which indicated that the blank TSGs and the CBD TSGs were almost nontoxic and nonirritating to the cilia. The CBD TSGs are safe and could be used for nasal administration (Fig. 4F).

The longer persistent vibration duration (PVD) and the higher percentage of persistent vibration (PPV) indicated higher safety and less irritation. The order of PVD and PPV was as follows: physiological saline (PS)>blank TSGs > low-dose CBD TSGs > medium-dose CBD TSGs > high-dose CBD TSGs > sodium deoxycholate. The PVD and PPV of the sodium deoxycholate group were significantly reduced ($P < 0.001$) compared with those of the PS group. The ciliary swinging time of the blank TSGs ($P < 0.001$) and CBD TSGs ($P < 0.001$) were not as long as those of the PS group, which indicated that the toxicity was greater than that of the PS group. However, their ciliary swinging time was significantly longer than that of the sodium deoxycholate group ($P < 0.001$). The PVD of blank TSGs, CBD

Table 1 Simulation of CBD TSG release *in vitro* with different mathematical models.

Math release model	Expression	Math release equation	R
Zero-order kinetic equation	$Q_n = K_0 \cdot t + a$	$Q_n = 1.4809t + 13.348$	0.8589
First-order kinetic equation	$\mathrm{Ln}\,(100 - Q_n) = -K_1 \cdot t + M$	$\mathrm{Ln}\,(100 - Q_n) = -0.0256t + 4.4608$	0.9028
Higuchi equation	$Q_n = k_H \cdot t^{1/2}$	$Q_n = 12.138t^{1/2} - 3.6851$	0.9485
Ritger−Peppas equation	$\mathrm{Ln}Q_n = n\mathrm{Ln}t + K$	$\mathrm{Ln}Q_n = 0.8959\ \mathrm{Ln}t + 1.3513$	0.9764

CBD, cannabidiol; TSGs, temperature-sensitive hydrogels.

TSGs of low, middle, and high doses were 4.9, 4.8, 4.6, and 4.3 times of the positive control-sodium deoxycholate, respectively. Thus, the blank TSGs and the low-, medium- and high-dose CBD TSGs are relatively safer and less toxic than the positive control (Table 2).

3.3. *Significant therapeutic effects of CBD TSGs on PTSD mice*

3.3.1. *Open field test to detect the spontaneous behavior of PTSD mice*

The open field test was used to evaluate the spontaneous behavior with the total distance, the entry number in the central area, the upright number, the upright time, and the feces number as the indicators[51]. The spontaneous behavior of the model mice was less active than that of healthy mice, with most of the time spent in the surrounding area. The positive sertraline and the low-, medium- and high-dose CBD TSGs treatments increased the activity in the central area of the open field. Among them, the therapeutic effect of high-dose CBD TSGs (30 mg/kg) was the most significant (Fig. 5A).

The total distance ($P < 0.001$) and the entry number in the central area ($P < 0.001$) of the PTSD model mice significantly were decreased compared with those of mice in the healthy group. In comparison, the total distance and the central entry number of mice in the sertraline ($P < 0.01$, $P < 0.01$), low- ($P < 0.01$, $P < 0.05$), medium- ($P < 0.001$, $P < 0.05$), and high-dose ($P < 0.001$, $P < 0.05$) nasally administered CBD TSGs groups were significantly increased compared with those of the model mice. However, blank TSGs could not improve the spontaneous behavior of PTSD mice in the open field. There were no statistical differences between the CBD TSGs groups and the sertraline group (Fig. 5B and C).

Upright behavior reflects the exploration degree of mice. The upright number ($P < 0.001$) and the upright time ($P < 0.001$) of the model mice were significantly reduced compared with those of the healthy mice, which indicated that their exploration spirit was poor. Sertraline ($P < 0.01$, $P < 0.01$) and medium- ($P < 0.05$, $P < 0.01$) and high-dose CBD TSGs ($P < 0.001$, $P < 0.001$) significantly increased the upright number and time among treated mice compared with the model mice. However, the blank TSGs group had no obvious effect. The high-dose CBD TSGs can significantly increase the total upright time of PTSD mice compared with the sertraline group ($P < 0.01$). Moreover, there were significant differences between the high-dose group and the low- ($P < 0.001$, $P < 0.001$), medium-dose ($P < 0.01$, $P < 0.05$) groups for the upright number and the upright time (Fig. 5D and E). This implied that CBD TSGs of high dose could improve the vitality and adventure activity significantly.

Feces counting is closely related to mental stress. Increased feces number implies more nervous condition. The number of feces number in the PTSD model mice was increased significantly ($P < 0.05$) compared with that of the healthy mice. Sertraline ($P < 0.01$) and low- ($P < 0.001$), medium- ($P < 0.001$), and high-dose CBD TSGs ($P < 0.001$) treatment could significantly reduce the feces number and decrease the tension compared with those in the model group. The blank TSGs group showed no improvement. However, there was no statistical differences between the different CBD TSGs groups and the sertraline group. In addition, the CBD TSGs groups of the low- ($P < 0.05$) and the medium-dose ($P < 0.05$) can significantly reduce the feces number of PTSD mice compared with the positive sertraline group (Fig. 5F).

All indicators from the open field test indicated that the PTSD model was successfully established, and sertraline and CBD TSGs could alleviate PTSD-like behavior of mice. In particular, a 30 mg/kg dose of CBD TSGs had an excellent effect of improving the spontaneous behavior and exploration spirit and reducing the metal stress of PTSD mice.

3.3.2. *Elevated plus maze test to evaluate the anxiety of PTSD mice*

The elevated plus maze is used to evaluate the anxiety of mice with the number of entering open arms, open arm latency and feces number as the indices, which also reflect anxiety conditions[52]. The healthy mice were active and moved freely between the open and the closed arms, and no anxiety was observed. Compared with the healthy mice, the PTSD model mice only moved in the closed arms. This demonstrated that the mice lacked security, and anxiety appeared. In comparison, sertraline and low-, medium- and high-dose CBD TSGs can increase the number of entering open arms and reduce the latency of open arms compared with the model group (especially high-dose CBD TSGs), which indicated that anxiety was alleviated. The blank TSGs group had no obvious improvement (Fig. 6A–C).

The feces number of the model mice increased significantly ($P < 0.01$) compared with those of the healthy mice. Sertraline ($P < 0.05$) and low- ($P < 0.001$), medium- ($P < 0.001$), and high-dose CBD TSGs ($P < 0.001$) can significantly reduce the feces number of PTSD mice compared with those in the model group, which indicated that sertraline and CBD TSGs can alleviate the mental tension of mice in the elevated plus maze. The blank TSGs had no obvious effects (Fig. 6D).

Overall, sertraline and CBD TSGs can attenuate anxiety behavior of PTSD mice. Among them, a high-dose of CBD TSGs had the best effect and was superior to the positive control of sertraline.

3.3.3. *Freezing behavior test to detect fear in PTSD mice*

Electrical stimulation could cause mice to become stiff and induce PTSD-like syndromes in a conditional fear box. Most model mice were frightened by the electrical pulse compared with the healthy ones. Sertraline and low-, medium- and high-dose nasally administered CBD TSGs could attenuate the fear behavior of mice

Table 2 Toxicity evaluation of the CBD TSGs with the ciliary swing.

Group	Persistent vibration duration (min)	Percentage of persistent vibration (%)
Saline group	657 ± 10.5	100
Sodium deoxycholate group	124.0 ± 10.6***	18.9 ± 1.6***
Blank TSGs group	607.0 ± 24.0***,###	92.4 ± 3.7***,###
10 mg/mL CBD TSGs group	593.7 ± 3.50***,###	90.4 ± 0.5***,###
20 mg/mL CBD TSGs group	570.0 ± 12.5***,###	86.8 ± 1.9***,###
30 mg/mL CBD TSGs group	534.7 ± 13.5***,###	81.4 ± 2.1***,###

Data are represented as mean ± SD ($n = 3$).
***$P < 0.001$ *vs.* the saline group.
###$P < 0.001$ *vs.* the sodium deoxycholate group.

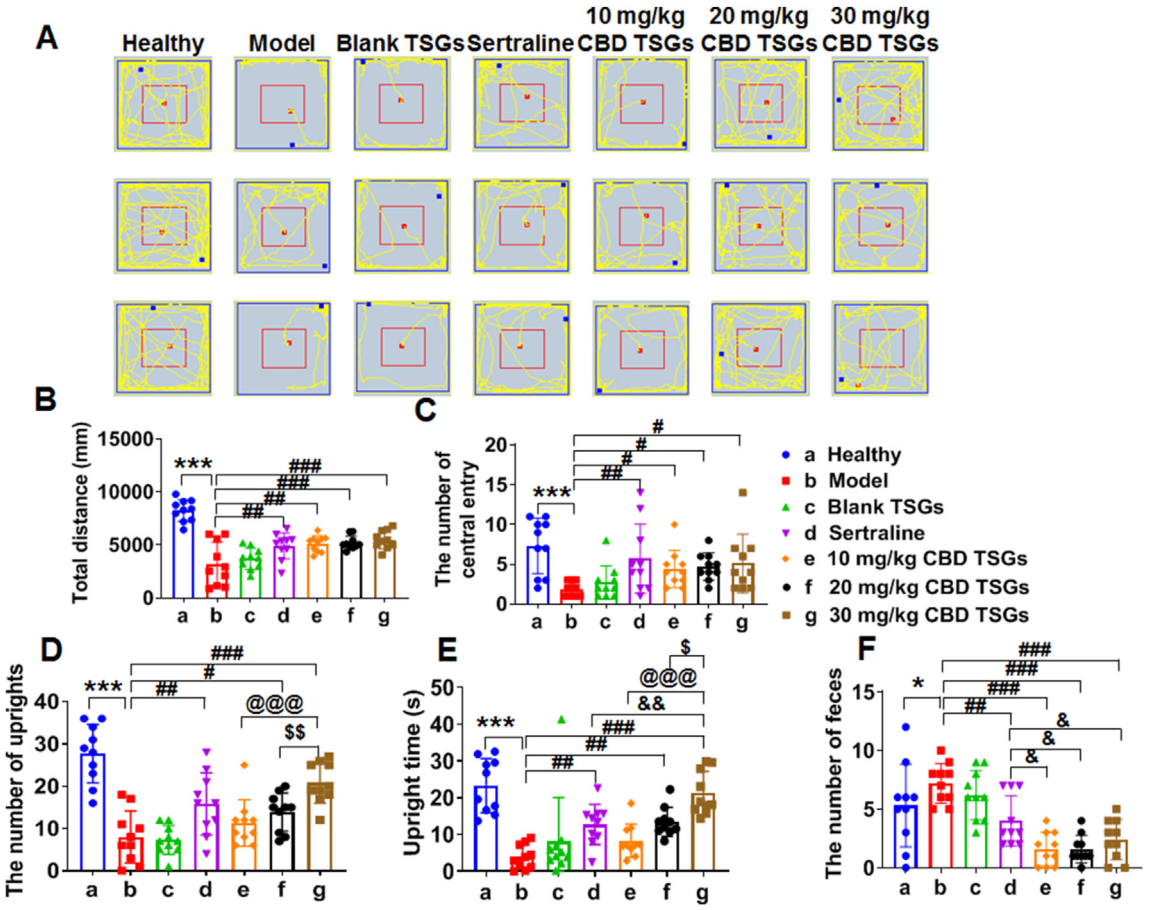

Figure 5 Comparison of the spontaneous behavior, the exploratory spirit and the mental tension of mice in each group. The trace map (A), total distance (B), number of central entries (C), number of uprights (D), upright time (E) and feces number (F) of mice in the open field box. Data are represented as mean ± SD ($n = 10$). *$P < 0.05$, ***$P < 0.001$ *vs.* the healthy group; $^{\#}P < 0.05$, $^{\#\#}P < 0.01$, $^{\#\#\#}P < 0.001$ *vs.* the model group; $^{\&}P < 0.05$, $^{\&\&}P < 0.01$ *vs.* the sertraline group; $^{@@@}P < 0.001$ *vs.* the low-dose CBD TSGs group; $^{\$}P < 0.05$, $^{\$\$}P < 0.01$ *vs.* the medium-dose CBD TSGs group.

compared with those in the model group. The efficacy of high-dose CBD TSGs was the most obvious (Fig. 7A).

The freezing behavior evaluation included two indices: the freezing time and the feces number. In detail, the freezing time ($P < 0.001$) of the model mice was increased significantly compared with that of the healthy mice, which indicated that the recurrence of the environment caused the mice to have a fear memory and induced PTSD-like syndromes. However, low- ($P < 0.001$), medium- ($P < 0.001$), and high-dose CBD TSGs ($P < 0.001$) could significantly reduce the freezing time compared with the model group without any treatments. High-dose CBD TSGs had the best effect, while the blank TSGs and the positive sertraline control led to no obvious improvement (Fig. 7B).

The feces number of the model mice increased significantly ($P < 0.01$) compared with that in the healthy group, which indicated that the mental tension was increased. Low- ($P < 0.001$), medium- ($P < 0.001$) and high-dose CBD TSGs ($P < 0.001$) could significantly reduce the feces number. However, the blank TSGs and the positive sertraline control did not show significant effects (Fig. 7C). In general, CBD TSGs could improve the freezing behavior and relieve the fearful mood of PTSD mice. Among them, a 30 mg/kg dose of CBD TSGs was the best.

3.3.4. Pathological evaluation of PTSD mice treated with the different strategies

In the healthy group, pyramidal neurons in the prefrontal cortex, hippocampus, and amygdala area were arranged densely and neatly with a regular karyotype and a large number of cell layers. In comparison, the cells in the prefrontal cortex, hippocampal CA1 region and amygdala of the model group were arranged sparsely with few cell layers and increased gaps. The nuclear karyotype was irregular, triangular or fusiform with uneven and irregular arrangement. In addition, nuclear shrinkage and deep staining in the model group indicated necrotic brain cells in PTSD mice and seriously damaged neurons, which indicated that PTSD can cause pathological changes in the prefrontal cortex, hippocampal CA1 region and amygdala areas. Compared with those from mice in the model group, the neurons in the pyramidal layer of the sertraline and medium- and high-dose CBD TSGs groups were arranged neatly and densely with the disappearance of nuclear shrinkage and deep staining, which indicated that the pathological changes in various brain regions of mice caused by PTSD were obviously alleviated with the treatment of sertraline and CBD TSGs.

For the CA2, CA3 and dentate gyrus (DG) areas of the hippocampus, there were no obvious differences between the

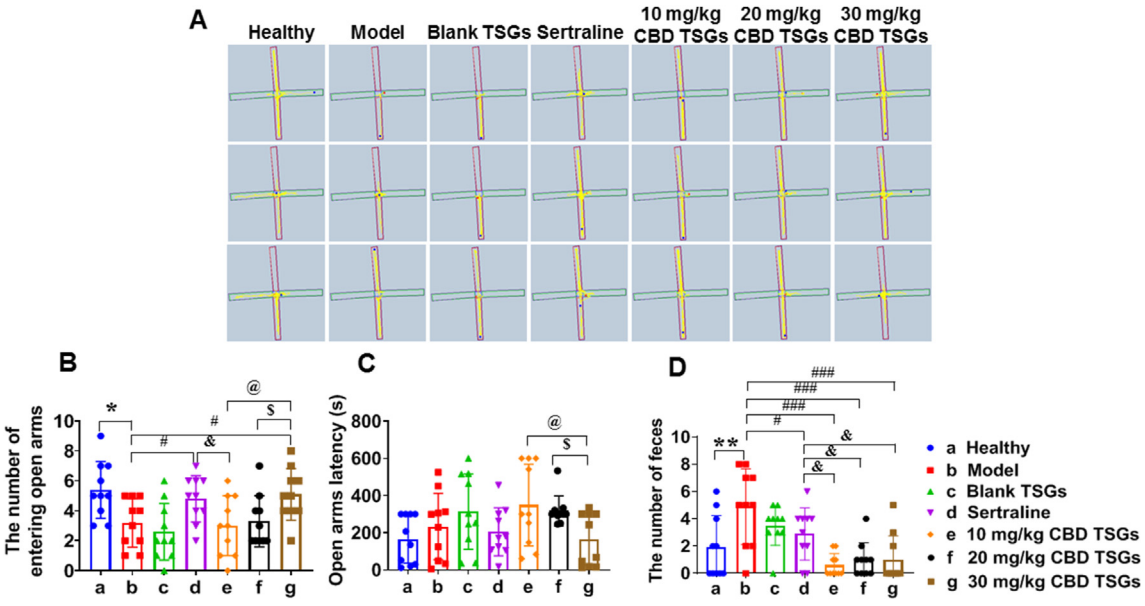

Figure 6 Comparison of the anxious behavior and the mental tension of mice in each group. The trace map (A), the number of entering open arms (B), open arms latency (C) and the feces number (D) of mice in the elevated plus maze. Data are represented as mean ± SD ($n = 10$). $^{**}P < 0.01$ *vs.* the healthy group; $^{\#}P < 0.05$, $^{\#\#\#}P < 0.001$ *vs.* the model group; $^{\&}P < 0.05$ *vs.* the sertraline group; $^{@}P < 0.05$ *vs.* the low-dose CBD TSGs group; $^{\$}P < 0.05$ *vs.* the medium-dose CBD TSGs group.

different groups. Therefore, it was preliminarily determined that the PTSD lesions mainly occurred in the prefrontal cortex, hippocampal CA1 area and amygdala of the brain (Fig. 8). PTSD can cause apoptosis of neurons in the prefrontal cortex, hippocampal CA1 region and amygdala of mice, which further caused the decline of memory and cognition. CBD TSGs could greatly alleviate the damage.

The expression of c-FOS can be used as a sign of neuronal activation by stimulation, which represents the neuronal excitability. The yellow staining of the prefrontal cortex, the CA1 region of the hippocampus, and the amygdala of the model group deepened compared with that of the healthy group, which indicated that the expression of c-FOS increased significantly. After administration for 10 days, sertraline and medium- and high-dose CBD TSGs could reduce the expression of c-FOS in the prefrontal cortex, hippocampal CA1 region and amygdala. High-dose CBD TSGs had the best effect with the lowest expression of c-FOS. The CA2, CA3, and DG areas of the hippocampus showed no significant differences in all groups. This result further indicated that the lesions in PTSD mice were mainly in the prefrontal cortex, the hippocampus CA1 region and the amygdala area, which were consistent with the H&E results (Fig. 9A).

The integrated optical density (IOD) of each zone and each group on immunohistochemistry was analyzed by Image-Pro Plus 6.0 (Media Cybernetics Co., Ltd., USA) software. In the CA1 area of the hippocampus, the expression of c-FOS in the model group was significantly upregulated ($P < 0.01$) compared with that in the healthy group. However, sertraline ($P < 0.05$), medium- ($P < 0.05$), and high-dose of CBD TSGs ($P < 0.01$) could significantly reduce the expression of c-fos compared with the model group.

In the prefrontal cortex of the brain, the expression of c-FOS in the model group was significantly increased ($P < 0.001$) compared with that in the healthy group, and sertraline ($P < 0.05$) and high-dose of CBD TSGs ($P < 0.01$) could significantly reduce the expression of c-FOS compared with the model group.

In the amygdala of the brain, the expression of c-FOS in the model group was significantly higher than that in the healthy group ($P < 0.001$). Compared with the model group, sertraline ($P < 0.01$), low- ($P < 0.05$), medium- ($P < 0.01$) and high-dose of CBD TSGs ($P < 0.001$) could significantly downregulate the expression of c-FOS. There was no significant difference in the CA2, CA3 and DG areas of the hippocampus among the groups (Fig. 9B).

3.3.5. *Decreased expression of TNF-α with CBD TSGs*

The inflammatory response is one of the representative pathogenic mechanisms of PTSD[53]. The TNF-α expression in the model group was significantly increased compared with that in the healthy group ($P < 0.001$). The positive sertraline control ($P < 0.01$) and low- ($P < 0.01$), medium- ($P < 0.001$), and high-dose CBD TSGs ($P < 0.001$) could significantly reduce the TNF-α content in the serum compared with the model group. Furthermore, high-dose CBD TSGs had the best effects. However, the blank TSGs failed to decrease the expression of TNF-α (Fig. 10A).

3.3.6. *Expression of the 5-HT1A receptor determined by WB*

The 5-HT1A receptor is a class of receptors of the monoamine system, which is associated with the various neuropsychiatric disorders, including depression, anxiety, and fear[54]. Higher 5-HT1A levels indicate a better mental condition. In detail, the expression of the 5-HT1A receptor in the model mice was significantly reduced compared with that in the healthy mice ($P < 0.001$). Sertraline ($P < 0.001$) and low- ($P < 0.001$), medium- ($P < 0.001$), and high-dose CBD TSGs ($P < 0.001$) could increase the expression of the 5-HT1A receptor compared with the model group (Fig. 10B and C). Among them, high-dose CBD TSGs had the most significant effect. PTSD could cause

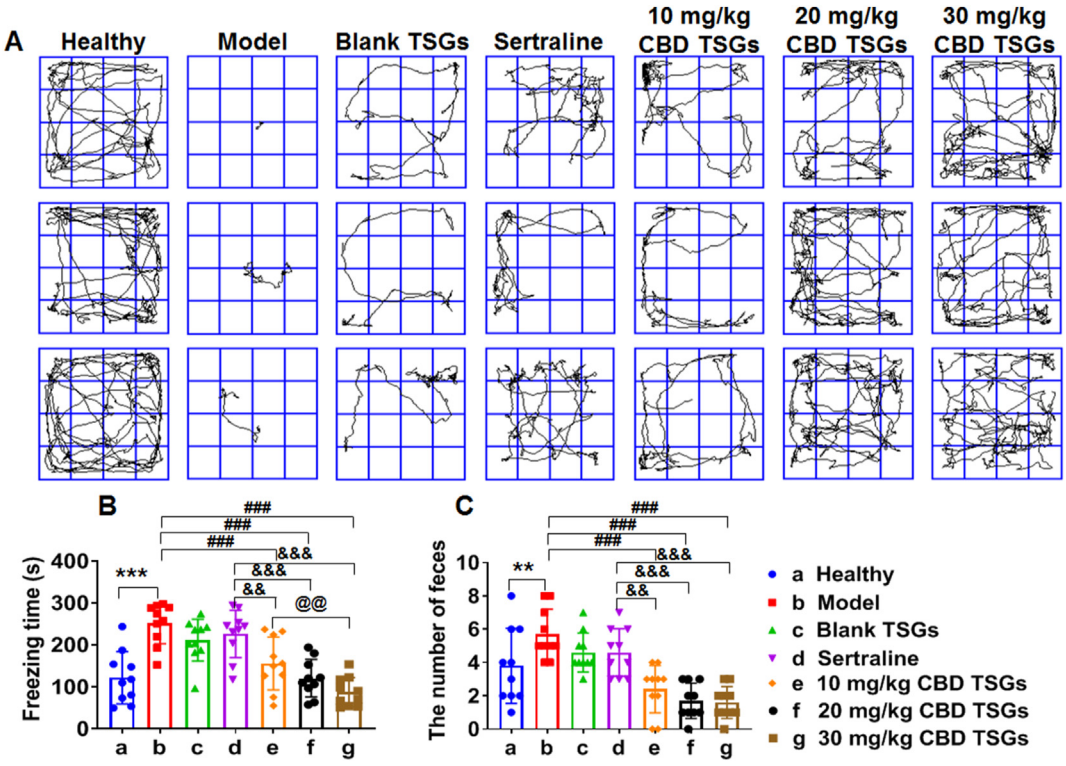

Figure 7 Comparison of the freezing behavior and the mental tension of mice in each group. The trace map (A), freezing time (B) and feces number (C) of mice in a conditional fear box. Data are represented as mean ± SD ($n = 10$). $^{**}P < 0.01$, $^{***}P < 0.001$ *vs.* the healthy group; $^{\#\#\#}P < 0.001$ *vs.* the model group; $^{\&\&}P < 0.01$, $^{\&\&\&}P < 0.001$ *vs.* the sertraline group; $^{@@}P < 0.01$ *vs.* the low-dose CBD TSGs group.

neurological dysfunction in mice. The mechanism may be related to the inhibition of the 5-HT1A receptor signaling pathway and could be reversed by nasal CBD TSGs.

3.4. High bioavailability and obvious brain-targeting effects of CBD ISGs by nasal administration

3.4.1. Quantification determination with mass spectrometry and chromatography method

For CBD, the *m/z* of the parent ion and the main fragment ion were 315.5 and 193.4, respectively (Fig. 11A). The parent ion and the main fragment ion of the internal standard (IS) propranolol were 260.1 and 116.0, respectively (Fig. 11B). The retention times of CBD and propranolol were 1.77 and 1.35 min, respectively. The endogenous substances in the blank plasma did not interfere with the determination of CBD and propranolol.

The linear correlation in different biological samples was determined, including plasma, brain and liver (Table 3).

3.4.2. Higher bioavailability and brain-targeting distribution of CBD by nasal administration

The T_{max} of CBD through oral administration was 1 h, and the nasal administration was 15 min. The C_{max} of nasal CBD administration was approximately 5 times that of the oral administration, and the area under the curve (AUC) of the nasal administration of CBD was approximately 7 times that of the oral administration (Fig. 11C and Table 4). With nasal administration, CBD could be absorbed faster and had a higher bioavailability than with the oral administration.

With nasal administration, CBD TSGs can quickly accumulate in the brain within 15 min compared with oral administration. The AUC of nasal administration was approximately 3 times that of oral administration (Fig. 11D and Table 4). It demonstrated that the nasal formulation could be directly absorbed into the brain, bypass the BBB and was absorbed less into the blood.

The liver is an important organ for metabolism of oral medicine. The CBD concentration in the liver after oral administration was higher than that after nasal administration, and the liver AUC after oral administration was slightly higher than that after nasal administration (Fig. 11E and Table 4).

Compared with the oral route, the relative bioavailability of CBD in blood, brain and liver was 693%, 313% and 77.9%, respectively (Table 4). CBD concentration in blood and brain was much higher than the oral route. In comparison, nasal CBD distributed little in liver than oral administration, which avoided the first-pass effect and had little toxicity on liver. Moreover, the T_{max} of the nasal route was much shorter than that of the oral route, which proved the quicker impact on PTSD.

4. Discussion

In this study, CBD was used as a model medicine to achieve brain targeting through nasal administration. The purpose was to develop a safe, effective and quality-controllable pharmaceutical preparation for the treatment of PTSD. First, the inclusion complex was prepared by freeze-drying to increase the aqueous solubility of CBD, and the inclusion rate was high. Subsequently, the

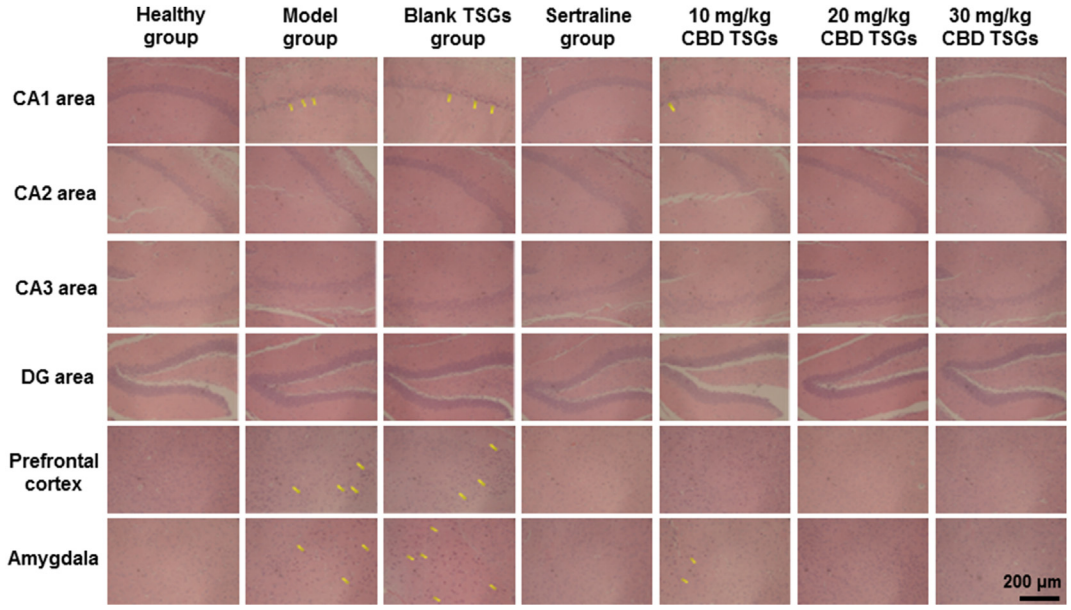

Figure 8 H&E staining of the prefrontal cortex, hippocampus and amygdala areas in the mice brains. Scale bar = 200 nm. The yellow arrows represent the pyknosis and deep staining parts of neurons.

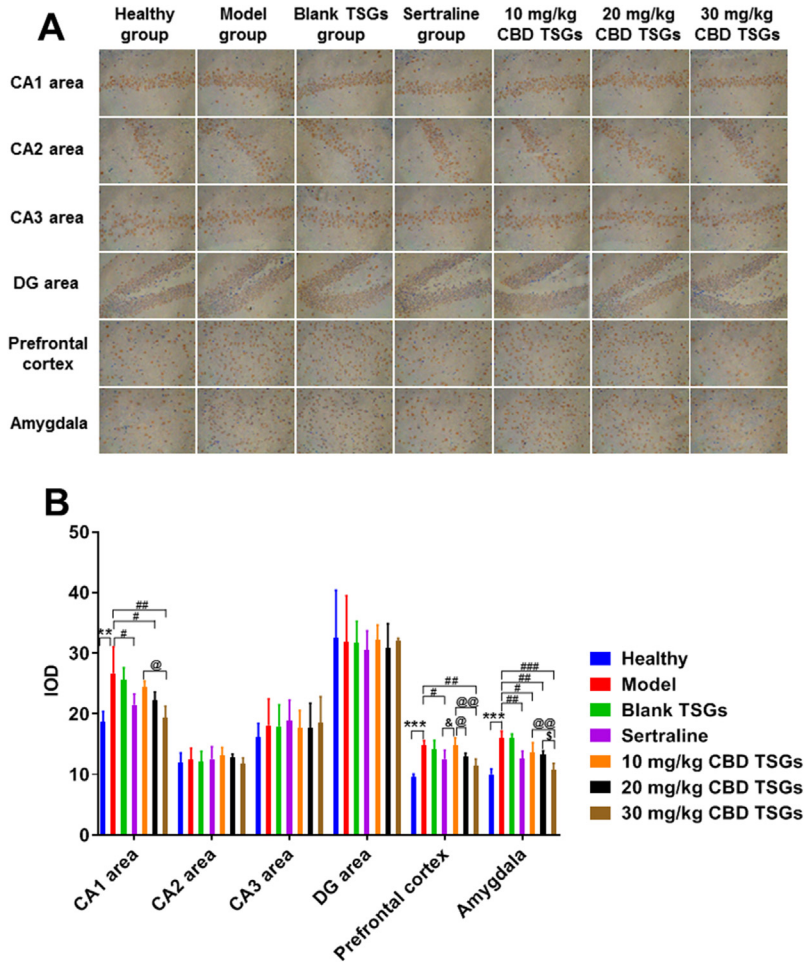

Figure 9 C-FOS expression of the prefrontal cortex, hippocampus and amygdala areas in the mice brains (A, scale bar = 100 nm). The integrated optical density (IOD) of the prefrontal cortex, hippocampus and amygdala area in the brains (B). Data are represented as mean ± SD ($n = 3$). $^{*}P < 0.05$, $^{**}P < 0.01$, $^{***}P < 0.001$ *vs.* the healthy group; $^{\#}P < 0.05$, $^{\#\#}P < 0.01$, $^{\#\#\#}P < 0.001$ *vs.* the model group; $^{\&}P < 0.05$ *vs.* the sertraline group; $^{@}P < 0.05$, $^{@@}P < 0.01$ *vs.* the low-dose CBD TSGs group; $^{\$}P < 0.05$ *vs.* the medium-dose CBD TSGs group.

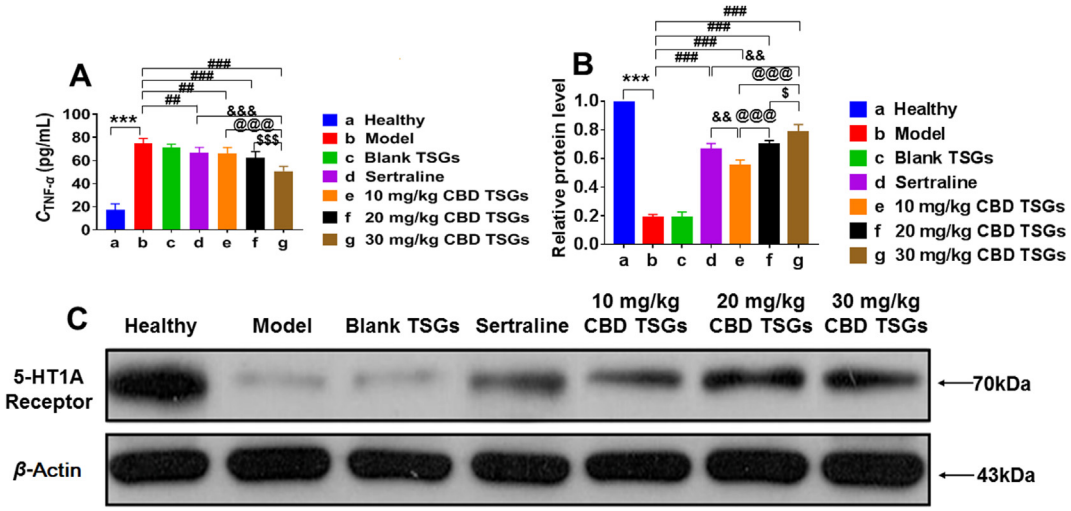

Figure 10 (A) Expression of TNF-α in the mice serum (Data are represented as mean ± SD, $n = 5$) (B and C) Expression of the 5-HT1A receptor in the hippocampus (Data are represented as mean ± SD, $n = 3$). $^{***}P < 0.001$ *vs.* the healthy group; $^{\#\#}P < 0.01$, $^{\#\#\#}P < 0.001$ *vs.* the model group; $^{\&\&}P < 0.01$, $^{\&\&\&}P < 0.001$ *vs.* the sertraline group; $^{@@@}P < 0.001$ *vs.* the low-dose CBD TSGs group; $^{\$}P < 0.05$, $^{\$\$\$}P < 0.001$ *vs.* the medium-dose CBD TSGs group.

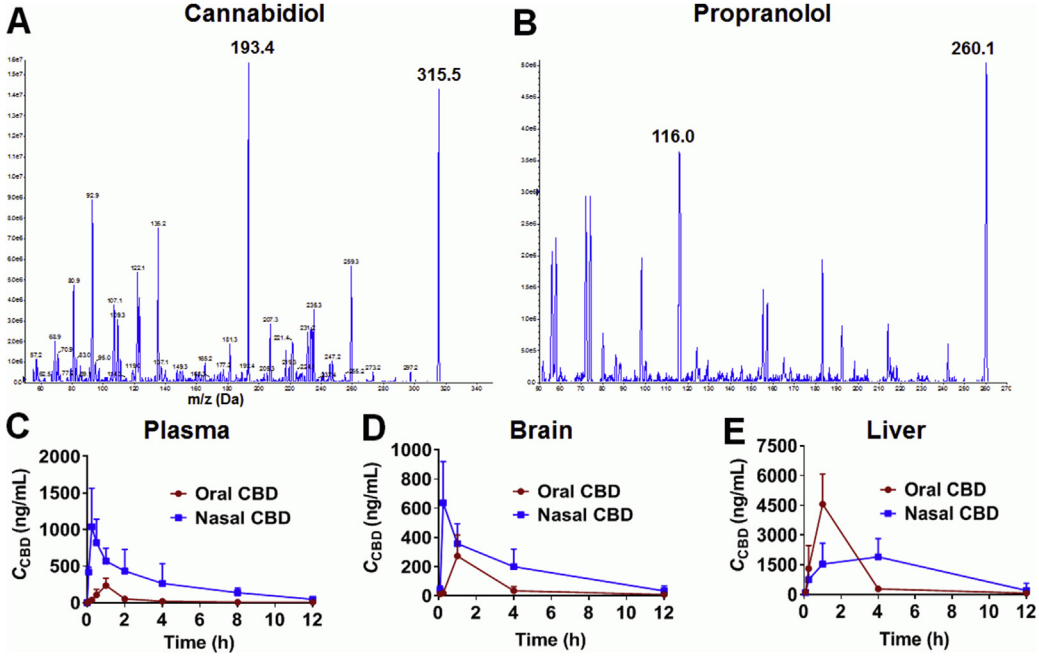

Figure 11 Mass spectra of CBD (A) and propranolol (B). CBD concentration−time curves of plasma (C), brain (D) and liver (E) after oral and nasal administration. Data are represented as mean ± SD ($n = 6$).

CBD inclusion complex was placed in a blank TSGs based on a poloxamer to obtain CBD TSGs, which had the advantages of strong adhesion, high bioavailability and high safety. This preparation is suitable for nasal administration and overcomes the shortcoming of traditional nasal preparations that have short residence times in the nasal cavity. Behavioral experiments have proven the therapeutic effect of CBD TSGs on PTSD. Pathological investigations have shown that the key brain areas related to PTSD are the prefrontal cortex, CA1 area of hippocampus and amygdala. The molecular biology initially clarified the mechanism of CBD TSGs in the treatment of PTSD. Finally, the pharmacokinetics experiments and brain and liver tissue distributions showed nasal administration had more advantages than oral administration. The T_{max} of nasal administration was shorter, and the medicine could accumulate in the brain to achieve a brain-targeting effect.

PTSD is a syndrome that develops after trauma related to the mental system. The open field test, elevated plus maze and freezing behavior test are the gold standards to reflect the effects of PTSD treatment. The open field test is one of the behavioral models used to study neurodegenerative diseases or brain damage; this test mainly evaluates spontaneous activity, exploratory

Table 3 Linear regression equation and linear range of the biological samples.

Sample	Linear regression equation	r	Linear range (ng/mL)
Blood	$A_{CBD}/A_{IS} = 0.0009C–0.0078$	0.9994	5−2000
Brain	$A_{CBD}/A_{IS} = 0.0019C + 0.0089$	0.9998	5−1000
Liver	$A_{CBD}/A_{IS} = 0.0023C + 0.0052$	0.9998	5−5000

Table 4 Pharmacokinetic parameters of CBD administered orally and nasally.

Parameter	T_{max}	C_{max}	AUC_{0-t}	MRT
Unit	h	ng/mL	h·ng/mL	h
Plasma–oral	1.00 ± 0.00	236.2 ± 97.35	428.02 ± 120.61	2.44 ± 0.48
Plasma–nasal	0.29 ± 0.10	1205 ± 471.3	2968.3 ± 705.13***	3.35 ± 0.65
Brain–oral	1.00 ± 0.00	273.0 ± 143.0	684.26 ± 346.02	2.05 ± 1.19
Brain–nasal	0.38 ± 0.31	647.0 ± 276.7	2138.8 ± 916.36*	2.91 ± 1.01
Liver–oral	0.88 ± 0.31	4631 ± 1420	13,723 ± 2841.4	1.60 ± 0.38
Liver–nasal	2.25 ± 1.94	2088 ± 815.2	10,685 ± 8412.6	3.52 ± 0.78
F_{blood}	693%			
F_{brain}	313%			
F_{liver}	77.9%			

Data are represented as the means ± SD, $n = 6$.
***$P < 0.001$ *vs.* the Plasma-oral; *$P < 0.05$ *vs.* the Brain–oral.
AUC, area under curve; MRT, mean residence time.
Relative blood bioavailability (%) = AUCnasal/AUCoral × 100 = 2968.3/428.02 × 100 = 93%.
Relative brain bioavailability (%) = AUCnasal/AUCoral × 100 = 2138.8/684.26 × 100 = 313%.
Relative liver bioavailability (%) = AUCnasal/AUCoral × 100 = 10,685/13,723 × 100 = 77.9%.

behavior and tension of experimental animals in an unfamiliar open environment. The elevated plus maze test is used to evaluate anxiety behavior, and the freezing behavior test is used to evaluate fearful behavior of animals in a conditional fear box. We have carried out experiments of all the above representative behavioral indicators. After the PTSD model was established by an unavoidable electric shock to the feet, the spontaneous behavior and exploratory spirit of the mice were significantly reduced, and their anxiety behavior, fearful emotion and tension levels were increased. After 10 days of administration, sertraline and CBD TSGs were found to improve their spontaneous behavior and exploratory spirit and alleviate their anxiety and fear emotions.

The prefrontal cortex is closely related to the regulation of emotions[55]. The hippocampus is mainly responsible for long-term learning and short-term memory, which is similar to the function of computer memory. The hippocampus can be divided into different subregions such as CA1, CA2, CA3 and DG[56]. The amygdala is a part of the limbic system and is related to emotional regulation, learning and memory[57]. In this study, H&E and c-FOS immunohistochemistry showed that the main lesion areas in PTSD were the prefrontal cortex, hippocampus CA1 area and amygdala, which seriously affected the level of emotion regulation, learning and memory.

The inflammatory response is one of the representative pathogenic mechanisms of PTSD. The expression of inflammatory factors in PTSD mice may increase, and TNF-α is an important indicator that reflects inflammation. The results showed that sertraline and CBD TSGs could reverse the increase in inflammatory factors caused by PTSD and reduce the expression of TNF-α. The 5-HT1A receptor is a type of receptor in the monoamine system and is associated with various neuropsychiatric diseases, including depression, anxiety, fear and so on[58]. The expression of the 5-HT1A receptor was determined to preliminarily show that PTSD can cause neurological dysfunction in mice. The therapeutic mechanism of CBD TSGs on PTSD may be related to the activation of the 5-HT1A receptor signaling pathway.

Compared with the nasal cavity, CBD with the oral pathway lost a lot due to the first pass effect. Therefore, the CBD blood concentration of oral administration was low, and AUC of nasal administration in brain and blood were much greater than that of oral administration. The distribution in the brain and liver proved that nasal administration had effective brain targeting and high bioavailability. First, the concentration of medicine in the brain is an important indicator for detecting brain targeting[59]. Nasal administration allowed CBD TSGs to quickly accumulate in the brain for approximately 15 min compared with oral administration. The AUC was approximately 3 times that of oral administration, which indicated that nasal administered CBD TSGs could be quickly absorbed into the brain, and the brain-targeting efficiency was higher with nasal administration than with oral administration. The preparation may penetrate or bypass the BBB and be absorbed into the brain after nasal administration. There are multiple nose−brain pathways, such as the olfactory nerve pathway and trigeminal nerve pathway. The various ways for entering the brain can increase the content of medicine in the brain. Second, the pharmacokinetic parameters indicated that CBD TSGs can reach peak concentration rapidly after nasal administration, and the time was approximately 15 min; in contrast, after oral administration, CBD TSGs reached the peak at 1 h, which indicated that CBD can be quickly absorbed into the blood through nasal administration. The nasal C_{max} was over 4 times that of orally administered CBD TSGs, and the nasal AUC was approximately 7 times that of orally administered CBD TSGs. The nasal mucosa has a large surface area and abundant capillaries[60], and this is advantageous for medicine absorption[61]. Third, the liver is an important organ involved in the metabolism of oral prescriptions[62], and the content of CBD in the liver was measured in this study. The CBD concentration in the liver after oral

administration was higher than that after nasal administration, with a slightly higher AUC. Nasal administration led to less distribution in the liver and allowed more CBD TSGs to enter the blood and brain. There is also another possibility that it was metabolized through other pathways, which needs further study.

The limitation of this study is that the stability of CBD TSGs was not investigated in the preparation. The most basic requirements of pharmaceutical preparations are safety, effectiveness and stability. If the preparation decomposes or deteriorates during production or storage, the efficacy of the medicine will be reduced. Later, the stability of CBD TSGs under extreme conditions of high temperature, high humidity and strong light irradiation will be evaluated. In addition, the mechanism of action of CBD TSGs on PTSD has not been studied clearly and totally. The influence of animals' sexuality on pharmacodynamics and pharmacokinetics is still unknown. The above limitations should be focused on in later research.

5. Conclusions

In this study, CBD TSGs were prepared according to the physiological conditions of the nasal cavity. A series of evaluations showed that the preparation was safe and effective, and the quality was controllable. Owing to the brain-targeting of nasal administration, CBD TSGs had a good therapeutic effect on PTSD. In summary, this study prepared a safe, effective, and quality-controlled brain-targeting preparation, which provides a new choice for the clinical treatment of PTSD. However, its mechanism of action still needs further research.

Acknowledgments

This paper was funded by the Beijing Municipal Natural Science Foundation, China (7202147 and 7172072, China).

Author contributions

Lulu Pang, Xu Jin, Lina Du and Yiguang Jin conceived and designed the research. Lulu Pang and Siqing Zhu are both the primary investigators of this experiment. They executed the experiments and undertook the data analysis and manuscript writing. Jinqiu Ma, Lin Zhu, Yijing Liu, Ge Ou, Ruiteng Li, Yaxin Wang, and Yi Liang were all involved in evaluating the anatomy of the animals. All of the authors have read and approved the final manuscript.

Conflicts of interest

The authors have no conflicts of interest to declare.

References

1. Grover S, Sahoo S, Chakrabarti S, Avasthi A. Post-traumatic stress disorder (PTSD) related symptoms following an experience of delirium. *J Psychosoc Res* 2019;**123**:109725.
2. Escobar JPH, Rafai SSA, Seshadri AJ, Weed C, Apoj M, Harlow A, et al. A multicenter study of post-traumatic stress disorder after injury: mechanism matters more than injury severity. *Surgery* 2018;**164**: 1246−50.
3. Dold M, Bartova L, Kautzky A, Souery D, Mendlewicz J, Serretti A, et al. The impact of comorbid post-traumatic stress disorder in patients with major depressive disorder on clinical features, pharmacological treatment strategies, and treatment outcomes—results from a cross-sectional European multicenter study. *Eur Neuropsychopharm* 2017; **27**:625−32.
4. Popescu M, Hughes JD, Popescu EA, Riedy G, DeGraba TJ. Reduced prefrontal MEG alpha-band power in mild traumatic brain injury with associated posttraumatic stress disorder symptoms. *Clin Neurophy* 2016;**127**:3075−85.
5. Fonkoue IT, Marvar PJ, Norrholm S, Li Y, Kankam ML, Jones TN, et al. Symptom severity impacts sympathetic dysregulation and inflammation in post-traumatic stress disorder (PTSD). *Brain Behav Immun* 2020;**83**:260−9.
6. Husky MM, Mazure CM, Masfety VK. Gender differences in psychiatric and medical comorbidity with post-traumatic stress disorder. *Compr Psychiatr* 2018;**84**:75−81.
7. Navas AF, Borja MEL, Aguilar VG, Arrebola JP, Andreu JMP, Perez J. Incidence and risk factors for post-traumatic stress disorder in a population affected by a severe flood. *Publ Health* 2017;**144**:96−102.
8. Yuan M, Pantazatos SP, Zhu H, Li Y, Miller JM, Falcone HR, et al. Altered amygdala subregion-related circuits in treatment-naïve post-traumatic stress disorder comorbid with major depressive disorder. *Eur Neuropsychopharm* 2019;**29**:1092−101.
9. Song D, Ge Y, Chen Z, Shang C, Guo Y, Zhao T, et al. Role of dopamine D3 receptor in alleviating behavioural deficits in animal models of post-traumatic stress disorder. *Prog Neuropsychopharm Biol Psychiatry* 2018;**84**:190−200.
10. Shang C, Guo Y, Yao JQ, Fang XX, Sun LJ, Jiang XY, et al. Rapid anti-PTSD-like activity of the TSPO agonist YL-IPA08: emphasis on brain GABA, neurosteroids and HPA axis function. *Behav Brain Res* 2020;**379**:112320.
11. Jin Y, Zeng P, An J, Xu J. Negative life events and post-traumatic stress disorder symptoms: a moderated mediation model of only-child status and depressive symptoms. *Publ Health* 2019;**172**:31−9.
12. Hough CM, Lindqvist D, Epel ES, Denis MS, Reus VI, Bersani FS, et al. Higher serum DHEA concentrations before and after SSRI treatment are associated with remission of major depression. *Psychoneuroendo* 2017;**77**:122−30.
13. Tripp JC, Norman SB, Kim HM, Venners MR, Martis B, Simon NM, et al. Residual symptoms of PTSD following sertraline plus enhanced medication management, sertraline plus PE, and PE plus placebo. *Psychiatr Res* 2020;**291**:113279.
14. VanDolah HJ, Bauer BA, Mauck KF. Clinicians' guide to cannabidiol and Hemp oils. *Mayo Clin Proc* 2019;**94**:1840−51.
15. Rajan TS, Giacoppo S, Iori R, Nicola GRD, Grassi G, Pollastro F, et al. Anti-inflammatory and antioxidant effects of a combination of cannabidiol and moringin in LPS-stimulated macrophages. *Fitoterapia* 2016;**112**:104−15.
16. Campos AC, Fogaca MV, Sonego AB, Guimarães FS. Cannabidiol, neuroprotection and neuropsychiatric disorders. *Pharmacol Res* 2016; **112**:119−27.
17. Tanasescu R, Constantinescu CS. Cannabinoids and the immune system: an overview. *Immunobiol* 2010;**215**:588−97.
18. Skelley JW, Deas CM, Curren Z, Ennis J. Use of cannabidiol in anxiety and anxiety-related disorders. *J Am Pharm Associ* 2020;**60**: 253−61.
19. Mitelpunk A, Kramer U, Kedem MH, Fink EZ, Orbach R, Chernuha V, et al. The safety, tolerability, and effectiveness of PTL-101, an oral cannabidiol formulation, in pediatric intractable epilepsy: a phase II, open-label, single-center study. *Epilepsy Behav* 2019;**98**:233−7.
20. Santos NAG, Martins NM, Sisti FM, Fernandes LS, Ferreira RS, Queiroz RHC, et al. The neuroprotection of cannabidiol against MPP^+-induced toxicity in PC12 cells involves trkA receptors, upregulation of axonal and synaptic proteins, neuritogenesis, and might be relevant to Parkinson's disease. *Toxicol Vitro* 2015;**30**:231−40.
21. Renarda J, Norris C, Rushlowa W, Laviolette SR. Neuronal and molecular effects of cannabidiol on the mesolimbic dopamine system: implications for novel schizophrenia treatments. *Neurosci Biobehav Rev* 2017;**75**:157−65.

22. HayateTanigami Yoneda M, Tabata Y, Echigo R, Kikuchi Y, Yamazaki M, et al. Endocannabinoid signaling from 2-arachidonoylglycerol to CB1 cannabinoid receptor facilitates reward-based learning of motor sequence. *Neurosci* 2019;**421**:1−16.
23. Sánchez AM, Warnault V, Romero SM, Pastor A, Mondragón N, Torre RDL, et al. Alcohol-induced conditioned place preference is modulated by CB2 cannabinoid receptors and modifies levels of endocannabinoids in the mesocorticolimbic system. *Pharmacol Biochem Behav* 2019;**183**:22−31.
24. Berardi A, Schelling G, Campolongo P. The endocannabinoid system and post traumatic stress disorder (PTSD): from preclinical findings to innovative therapeutic approaches in clinical settings. *Pharmacol Res* 2016;**111**:668−78.
25. Waldinger MD, RSv Coevorden, Schweitzer DH, Georgiadis J. Penile anesthesia in Post SSRI Sexual Dysfunction (PSSD) responds to low-power laser irradiation: a case study and hypothesis about the role of transient receptor potential (TRP) ion channels. *Eur J Pharmacol* 2015;**753**:263−8.
26. Long Z, Duan X, Xie B, Du H, Li R, Xu Q, et al. Altered brain structural connectivity in post-traumatic stress disorder: a diffusion tensor imaging tractography study. *J Affect Disord* 2013;**150**:798−806.
27. Noack PH, Nikitovic D, Neagu M, Docea AO, Engin AB, Gelperina S, et al. The blood−brain barrier and beyond: nano-based neuropharmacology and the role of extracellular matrix. *Nanomed Nanotech Biol Med* 2019;**17**:359−79.
28. Jung B, Huh H, Lee E, Han M, Park J. An advanced focused ultrasound protocol improves the blood–brain barrier permeability and doxorubicin delivery into the rat brain. *J Control Release* 2019;**315**:55−64.
29. Maria ARS, Walter FR, Valkai S, Brás AR, Mészáros M, Kincses A, et al. Lidocaine turns the surface charge of biological membranes more positive and changes the permeability of blood–brain barrier culture models. *Biochim Biophys Acta Biomembr* 2019;**1861**:1579−91.
30. Chen J, Wang X, Wang J, Liu G, Tang X. Evaluation of brain-targeting for the nasal delivery of ergoloid mesylate by the microdialysis method in rats. *Eur J Pharm Biopharm* 2008;**68**:694−700.
31. Westin U, Piras E, Jansson B, Bergström U, Dahlin M, Brittebo E, et al. Transfer of morphine along the olfactory pathway to the central nervous system after nasal administration to rodents. *Eur J Pharm Sci* 2005;**24**:565−73.
32. Li M, Zhao M, Yao Fu YL, Gong T, Zhang Z, Sun X. Enhanced intranasal delivery of mRNA vaccine by overcoming the nasal epithelial barrier *via* intra- and paracellular pathways. *J Control Release* 2016;**228**:9−19.
33. Liu Y, Yang F, Feng L, Yang L, Chen L, Wei G. In vivo retention of poloxamer-based *in situ* hydrogels for vaginal application in mouse and rat models. *Acta Pharm Sin B* 2017;**7**:502−9.
34. Saingam W, Sakunpak A. Development and validation of reverse phase high performance liquid chromatography method for the determination of delta-9-tetrahydrocannabinol and cannabidiol in oromucosal spray from cannabis extract. *Revista Brasileira de Farmacognosia* 2018;**28**:669−72.
35. Chunshom N, Chuysinuan P, Thanyacharoen T, Techasakul S, Ummartyotin S. Development of gallic acid/cyclodextrin inclusion complex in freeze-dried bacterial cellulose and poly (vinyl alcohol) hydrogel: controlled-release characteristic and antioxidant properties. *Mater Chem Phys* 2019;**232**:294−300.
36. Chen W, Li R, Zhu S, Ma J, Pang L, Ma B, et al. Nasal timosaponin BII dually sensitive *in situ* hydrogels for the prevention of Alzheimer's disease induced by lipopolysaccharides. *Int J Pharm* 2020;**578**:119115.
37. Bittencourt VCE, Moreira AMdS, Silva JGd, Gomides AFdF, Rodrigues CV, Kelmann RG, et al. Hydrophobic nanoprecipitates formed by benzoylphenylureas and β-cyclodextrin inclusion compounds: synthesis, characterization and toxicity against aedes aegypti larvae. *Heliyon* 2019;**5**:e02013.
38. Oliveira CXd NSFerreira, Mota GVS. A DFT study of infrared spectra and Monte Carlo predictions of the solvationshell of praziquantel and β-cyclodextrin inclusion complex in liquid water. *Spectrochim Acta A Mol Biomol Spectr* 2016;**153**:102−7.
39. Yao Q, You B, Zhou S, Chen M, Wang Y, Li W. Inclusion complexes of cypermethrin and permethrinwith monochlorotriazinyl-beta-cyclodextrin: a combined spectroscopy, TG/DSC and DFT study. *Spectrochim Acta A Mol Biomol Spectr* 2014;**117**:576−86.
40. Hao J, Zhao J, Zhang S, Tong T, Zhuang Q, Jin K, et al. Fabrication of an ionic-sensitive *in situ* gel loaded with resveratrol nanosuspensions intended for direct nose-to-brain delivery. *Colloids Surf B Biointerfaces* 2016;**147**:376−86.
41. Swain GP, Patel S, Gandhi J, Shah P. Development of moxifloxacin hydrochloride loaded *in-situ* gel for the treatment of periodontitis: *in-vitro* drug release study and antibacterial activity. *J Oral Biol Craniofacial Res* 2019;**9**:190−200.
42. Zhang L, Pang L, Zhu S, Ma J, Li R, Liu Y, et al. Intranasal tetrandrine temperature-sensitive *in situ* hydrogels for the treatment of microwave-induced brain injury. *Int J Pharm* 2020;**583**:119384.
43. Maymon N, Aviv TMZ, Sabban EL, Akirav I. Neuropeptide Y and cannabinoids interaction in the amygdala after exposure to shock and reminders model of PTSD. *Neuropharm* 2020;**162**:107804.
44. Shimizu T, Minami C, Mitani A. Effect of electrical stimulation of the infralimbic and prelimbic cortices on anxiolytic-like behavior of rats during the elevated plus-maze test, with particular reference to multiunit recording of the behavior-associated neural activity. *Behav Brain Res* 2018;**353**:168−75.
45. Liu L, Liu H, Hou Y, Shen J, Qu X, Liu S. Temporal effect of electroacupuncture on anxiety-like behaviors and c-Fos expression in the anterior cingulate cortex in a rat model of post-traumatic stress disorder. *Neurosci Lett* 2019;**711**:134432.
46. Chhibber A, Woody SK, Rumi MAK, Soares MJ, Zhao L. Estrogen receptor β deficiency impairs BDNF−5-HT2A signaling in the hippocampus of female brain: a possible mechanism for menopausal depression. *Psychoneuroendo* 2017;**82**:107−16.
47. Palazzoli F, Citti C, Licata M, Vilella A, Manca L, Zoli M, et al. Development of a simple and sensitive liquid chromatography triple quadrupole mass spectrometry (LC−MS/MS) method for the determination of cannabidiol (CBD), 9-tetrahydrocannabinol (THC) and its metabolites in rat whole blood after oral administration of a single high dose of CBD. *J Pharm Biomed Anal* 2018;**150**:25−32.
48. Song S, Gao K, Niu R, Yi W, Zhang J, Gao C, et al. Binding behavior, water solubility and *in vitro* cytotoxicity of inclusion complexes between ursolic acid and amino-appended β-cyclodextrins. *J Mol Liquids* 2019;**296**:111993.
49. Su W, Liang Y, Meng Z, Chen X, Lu M, Han X, et al. Inhalation of tetrandrine-hydroxypropyl-β-cyclodextrin inclusion complexes for pulmonary fibrosis treatment. *Mol Pharm* 2020;**17**:1596−607.
50. Xiang Y, Long Y, Yang Q, Zheng C, Cui M, Ci Z, et al. Pharmacokinetics, pharmacodynamics and toxicity of baicalin liposome on cerebral ischemia reperfusion injury rats *via* intranasal administration. *Brain Res* 2020;**1726**:146503.
51. Lv Y, Li K, Wan J, Li C, Song X. Effects of flower volatiles from two liana species on spontaneous behavior of mice. *Acta Ecol Sin* 2020;**40**:90−6.
52. Cipriano AC, Gomes KS, Souza RLN. CRF receptor type 1 (but not type 2) located within the amygdala plays a role in the modulation of anxiety in mice exposed to the elevated plus maze. *Horm Behav* 2016;**81**:59−67.
53. Olff M, Mv Zuiden. Neuroendocrine and neuroimmune markers in PTSD: pre-, peri- and post-trauma glucocorticoid and inflammatory dysregulation. *Curr Opin in Psycho* 2017;**14**:132−7.
54. Isooka N, Miyazaki I, Kikuoka R, Wada K, Nakayama E, Shin K, et al. Dopaminergic neuroprotective eects of rotigotine *via* 5-HT1A receptors: possibly involvement of metallothionein expression in astrocytes. *Neurochem Int* 2020;**132**:104608.
55. Ozawa S, Kanayama N, Hiraki K. Emotion-related cerebral blood flow changes in the ventral medial prefrontal cortex: an NIRS study. *Brain Cognit* 2019;**134**:21−8.

56. Sagarkar S, Balasubramanian N, Mishra S, Choudhary AG, Kokare DM, Sakharkar AJ. Repeated mild traumatic brain injury causes persistent changes in histone deacetylase function in hippocampus: implications in learning and memory deficits in rats. *Brain Res* 2019;**1711**:183−92.
57. Butler CW, Wilson YM, Mills SA, Gunnersen JM, Murphy M. Evidence that a defined population of neurons in lateral amygdala is directly involved in auditory fear learning and memory. *Neurobiol Learn Mem* 2020;**168**:107139.
58. Cai CY, Wu HY, Luo CX, Zhu DY, Zhang Y, Zhou QG, et al. Extracellular regulated protein kinase is critical for the role of 5-HT1a receptor in modulating nNOS expression and anxiety-related behaviors. *Behav Brain Res* 2019;**357**−**358**:88−97.
59. Hong L, Li X, Bao Y, Duvall CL, Zhang C, Chen W, et al. Preparation, preliminary pharmacokinetic and brain targeting study of metformin encapsulated W/O/W composite submicron emulsions promoted by borneol. *Eur J Pharm Sci* 2019;**133**:160−6.
60. Buchthal B, Weiss U, Bading H. Post-injury nose-to-brain delivery of activin A and erpinB2 reduces brain damage in a mouse stroke model. *Mol Ther* 2018;**26**:2357−65.
61. Shingaki T, Hidalgo IJ, Furubayashi T, Sakane T, Katsumi H, Yamamoto A, et al. Nasal delivery of P-gp substrates to the brain through the nose brain pathway. *Drug Meta Pharmaco* 2011;**26**:248−55.
62. Lu H, Yuan X, Zhang Y, Han M, Liu S, Han K, et al. HCBP6 deficiency exacerbates glucose and lipid metabolism disorders in non-alcoholic fatty liver mice. *Biomed Pharmacother* 2020;**129**:110347.